

Laser Flash Photolysis and Matrix Isolation Studies of Ru[R₂PCH₂CH₂PR₂]₂H₂ (R = C₂H₅, C₆H₅, C₂F₅): Control of Oxidative Addition Rates by Phosphine Substituents

Leroy Cronin,[†] M. Carmen Nicasio,[†] Robin N. Perutz,^{*,†} R. Greg Peters,[‡] Dean M. Roddick,[‡] and Michael K. Whittlesey[†]

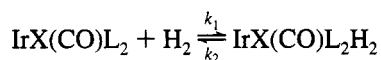
Contribution from the Department of Chemistry, University of York, Heslington, York, YO1 5DD, U.K., and Department of Chemistry, Box 3838, University of Wyoming, Laramie, Wyoming 82071

Received June 19, 1995[⊗]

Abstract: The photochemistry of ruthenium hydrides Ru(depe)₂H₂, *cis*-Ru(dppe)₂H₂ and *cis*-Ru(dfepe)₂H₂ [depe = Et₂PCH₂CH₂PEt₂, dppe = Ph₂PCH₂CH₂PPh₂, dfepe = (C₂F₅)₂PCH₂CH₂P(C₂F₅)₂] has been studied by matrix isolation at 12 K and laser flash photolysis at ambient temperature. Both techniques yield the 4-coordinate 16-electron RuP₄ species. The ethyl and phenyl species, Ru(depe)₂ and Ru(dppe)₂, exhibit very similar UV–visible spectra to Ru(dmpe)₂ [Ru(depe)₂ 475, 580, 735 nm; Ru(dppe)₂ 465, 550, 760 nm in solution]. The spectrum of Ru(dfepe)₂ is blue-shifted relative to the others (380, 450, 620 nm). The comparison of the spectra with that of [Rh(dppe)₂]⁺ conclusively establishes a square-planar structure for Ru(depe)₂ and Ru(dppe)₂. The rates of reaction with added ligands are extremely sensitive to substituent. The rate constants for reaction with H₂ are Ru(dfepe)₂ 2.0 × 10⁵, Ru(dppe)₂ 2.4(2) × 10⁷, Ru(depe)₂ 4.0(4) × 10⁸ dm³ mol⁻¹ s⁻¹ compared to 6.8 × 10⁹ dm³ mol⁻¹ s⁻¹ for Ru(dmpe)₂. For reaction with CO, the rate constants are Ru(dfepe)₂ 1.1 × 10⁴, Ru(dppe)₂ 1.0(2) × 10⁷, Ru(depe)₂ 9.1(7) × 10⁷ dm³ mol⁻¹ s⁻¹ compared to 4.6 × 10⁹ dm³ mol⁻¹ s⁻¹ for Ru(dmpe)₂. Thus reactivity increases in the order Ru(dfepe)₂ < Ru(dppe)₂ < Ru(depe)₂ < Ru(dmpe)₂ with an overall span of a factor of 34 000 for reaction with H₂ and 418 000 for reaction with CO. The rate constants for reaction of Ru(depe)₂ with C₂H₄ and Et₃SiH, and for reaction of Ru(dppe)₂ with C₂H₄ have also been determined.

Introduction

The oxidative addition of hydrogen by transition metal phosphine complexes represents a key step in many homogeneous catalytic reaction pathways, such as hydrogenation and hydroformylation.¹ Numerous mechanistic studies have been reported for H₂ addition to square planar d⁸ complexes, particularly derivatives of Vaska's complex, IrX(CO)L₂ (X = halide, L = tertiary phosphine).



Kinetic studies have revealed that both the rate of the forward step *k*₁ and reverse step *k*₂ are sensitive to the nature of the halide² and also the phosphine.³ The rate of H₂ addition decreases in the order P(*p*-MeOC₆H₄)₃ > PPh₃ ≈ PEt₃ > PⁱPr₃ > PCy₃; the rates depend on both steric and electronic properties of the substituent.

Studies of H₂ addition by conventional methods are necessarily limited to less reactive complexes. If the coordinatively unsaturated complex is formed only as a reactive intermediate,

other techniques are required.⁴ It is such species which exhibit the highest reactivity and are capable, for instance, of inserting into C–H bonds. We have recently employed laser flash photolysis to determine⁵ rate constants for the oxidative addition of H₂ to the coordinatively unsaturated d⁸ species, Fe(dmpe)₂ and Ru(dmpe)₂ (dmpe = Me₂PCH₂CH₂PMe₂), which are produced upon photolysis of the dihydride precursors *cis*-M(dmpe)₂H₂. The rate constant for the ruthenium species is close to the diffusion-controlled limit and, more remarkably, is 7500 times faster than for the iron species. Ru(dmpe)₂ has a striking three-band visible spectrum, which we associated with a square-planar geometry, whereas Fe(dmpe)₂ is postulated to have a butterfly structure. Both species are known to react with C–H bonds in solution; other group 8 metal complexes of the form ML₄ (L = phosphine) are known to undergo similar reactions.⁶

In an effort to probe the influence of the bidentate phosphine ligand on the structure and reactivity of the ruthenium center, we now report studies on the [(C₂H₅)₂PCH₂CH₂P(C₂H₅)₂]

(4) (a) Wink, D. A.; Ford, P. C. *J. Am. Chem. Soc.* **1985**, *107*, 1794. (b) Wink, D. A.; Ford, P. C. *J. Am. Chem. Soc.* **1986**, *108*, 4838. (c) Wink, D. A.; Ford, P. C. *J. Am. Chem. Soc.* **1987**, *109*, 436.

(5) (a) Hall, C.; Jones, W. D.; Mawby, R. J.; Osman, R.; Perutz, R. N.; Whittlesey, M. K. *J. Am. Chem. Soc.* **1992**, *114*, 7425. (b) Whittlesey, M. K.; Mawby, R. J.; Osman, R.; Perutz, R. N.; Field, L. D.; Wilkinson, M. P.; George, M. W. *J. Am. Chem. Soc.* **1993**, *115*, 8627.

(6) (a) Baker, M. V.; Field, L. D. *J. Am. Chem. Soc.* **1986**, *108*, 7433. (b) Baker, M. V.; Field, L. D. *J. Am. Chem. Soc.* **1987**, *109*, 4838. (c) Jones, W. D.; Kosar, W. P. *J. Am. Chem. Soc.* **1986**, *108*, 5640. (d) Hsu, G. C.; Kosar, W. P.; Jones, W. D. *Organometallics* **1994**, *13*, 385. For representative examples of C–H activation reactions by ML₄ complexes, see: (e) Hartwig, J. F.; Andersen, R. A.; Bergman, R. G. *J. Am. Chem. Soc.* **1991**, *113*, 6492. (f) Hartwig, J. F.; Andersen, R. A.; Bergman, R. G. *Organometallics* **1991**, *10*, 1710. (g) Koola, J. D.; Roddick, D. M. *J. Am. Chem. Soc.* **1991**, *113*, 1450. (h) Shinomoto, R. S.; Desrosiers, P. J.; Harper, T. G. P.; Flood, T. C. *J. Am. Chem. Soc.* **1990**, *112*, 704.

[†] University of York.

[‡] University of Wyoming.

[⊗] Abstract published in *Advance ACS Abstracts*, September 15, 1995.

(1) (a) Collman, J. P.; Hegedus, L. S.; Norton, J. R.; Finke, R. G. *Principles and Applications of Organotransition Metal Chemistry*; University Science Books: Mill Valley, CA, 1987. (b) Masters, C. *Homogeneous Transition Metal Catalysis – a gentle art*; Chapman and Hall: London, 1981.

(2) Chock, P. B.; Halpern, J. *J. Am. Chem. Soc.* **1966**, *88*, 3511.

(3) (a) Brady, R.; De Camp, W. H.; Flynn, B. R.; Schneider, M. L.; Scott, J. D.; Vaska, L.; Werneke, M. F. *Inorg. Chem.* **1975**, *14*, 2669. (b) Ugo, R.; Pasini, A.; Fusi, A.; Cenini, S. *J. Am. Chem. Soc.* **1972**, *94*, 7364. (c) Strohmeier, W.; Onoda, T. *Z. Naturforsch.* **1969**, *24B*, 515. (d) Strohmeier, W.; Onoda, T. *Z. Naturforsch.* **1968**, *23B*, 1527.

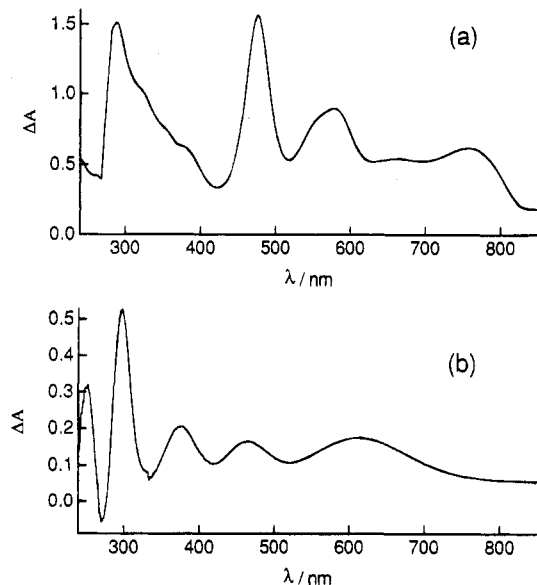


Figure 1. (a) UV-visible difference spectrum following 15-min broad-band photolysis of $\text{Ru}(\text{depe})_2\text{H}_2$ in an argon matrix at 12 K and (b) UV-visible difference spectrum following filtered UV photolysis ($\lambda = 234\text{--}376$ nm, 30 min) of $\text{Ru}(\text{dfepe})_2\text{H}_2$ in an argon matrix at 12 K. The spectra were obtained by subtraction of the deposition spectra from those recorded after photolysis.

(abbreviated to "depe"), $[(\text{C}_6\text{H}_5)_2\text{PCH}_2\text{CH}_2\text{P}(\text{C}_6\text{H}_5)_2]$ ("dppe"), and $[(\text{C}_2\text{F}_5)_2\text{PCH}_2\text{CH}_2\text{P}(\text{C}_2\text{F}_5)_2]$ ("dfepe") analogues of $\text{Ru}(\text{dmpe})_2\text{H}_2$. This choice of ligands allows us to change the electronic properties from an electron-rich metal center (dmpe/depe) to an electron-poor case (dfepe) and also to alter the steric bulk (cone angles: dmpe = 107° , depe = 115° , dppe = 125° , dfepe = 129°).⁷ The results provide strong evidence that all the $\text{Ru}(\text{drpe})_2$ (drpe = dmpe, depe, dppe, dfepe) complexes have structures close to square planar and demonstrate remarkable changes in rates of reaction according to substituent.

Results

1. Matrix Photochemistry. a. $\text{Ru}(\text{depe})_2\text{H}_2$ in Inert Matrices. A sample of $\text{Ru}(\text{depe})_2\text{H}_2$ (3:1 *cis/trans* mixture by ^1H NMR) was cocondensed with argon. The IR spectrum recorded at 12 K showed a broad band at 1825 cm^{-1} for the Ru-H stretching mode and bands at lower frequency associated with the depe ligand.⁸ The UV-visible spectrum of this white compound was broad and featureless.

Broad-band UV photolysis of the matrix (15 min) resulted in a 63% depletion of the hydride band and the appearance of no new features in the same region, therefore, excluding cyclometalation of the depe ligand. The UV-visible spectrum recorded after photolysis showed new absorption bands at 286, 476, 573, and 757 nm (Figure 1a, Table 1). Long wavelength photolysis designed to irradiate selectively on the red side of the band at 476 nm ($\lambda = 490\text{--}509$ nm, 60 min) resulted in a small depletion of all the UV-visible bands and a growth in the intensity of the metal hydride stretch in the IR spectrum. We therefore associate all the UV-visible bands with a single product. The positions of the UV-visible bands of the photoproduct were identical when the matrix host was changed from argon to methane (Table 1).

(7) (a) Ernst, M. F.; Roddick, D. M. *Organometallics* **1990**, *9*, 1586. (b) Tolman, C. A. *Chem. Rev.* **1977**, *77*, 313.

(8) IR bands for $\text{Ru}(\text{depe})_2\text{H}_2$ in an argon matrix at 12 K (ν , cm^{-1}): 2965 m, 2939 m, 2909 m, 2883 m, 1838 m, 1825 m, 1818 m, 1465 m, 1457 m, 1417 m, 1046 m, 1039 m, 1027 m, 998 w, 975 w, 869 w, 807 m, 762 m, 755 m, 736 m, 695 m.

b. $\text{cis-Ru}(\text{dfepe})_2\text{H}_2$ in Inert Matrices. The IR spectrum of $\text{cis-Ru}(\text{dfepe})_2\text{H}_2$ in an argon matrix at 12 K displayed a broad, weak band for $\nu(\text{Ru-H})$ at 1980 cm^{-1} (cf. 1990 cm^{-1} in nujol)^{6g} and vibrations due to the dfepe ligand at lower frequency.⁹ The UV-visible spectrum recorded in the same matrix showed bands at 272 and 235 nm.

Filtered UV photolysis ($\lambda = 234\text{--}376$ nm, 30 min) resulted in 60% depletion of the hydride band of the starting material. No new Ru-H bands were observed in the IR spectrum and very little change was observed at lower frequency. Interactive subtraction indicated the presence of new product bands overlapping with starting material bands in the lower frequency region of the IR spectrum associated with the dfepe modes. The UV-visible spectrum recorded after photolysis showed depletion of the two bands at 272 and 235 nm and the appearance of new bands at 251, 297, 375, 461, and 611 nm (Figure 1b, Table 1). Visible photolysis (either $\lambda = 420\text{--}450$ nm or $\lambda = 475\text{--}508$ nm, 150 min) resulted in slight shifts in all of the visible bands. No regeneration of intensity in the Ru-H stretching mode of the starting material was observed in the IR spectrum.

A change of the matrix host from argon to methane resulted in the parallel observations with virtually no difference in λ_{max} for the absorption bands of the photoproduct.

c. Photolysis of $\text{Ru}(\text{depe})_2\text{H}_2$ and $\text{Ru}(\text{dfepe})_2\text{H}_2$ in CO-Doped Matrices. Photolysis of the depe complex in a 1.7% CO/Ar matrix ($\lambda > 200$ nm, 5 min) resulted in the formation of a new band at 1850 cm^{-1} , which was assigned to $\nu(\text{CO})$ of $\text{Ru}(\text{depe})_2\text{CO}$ by comparison with solution IR data (see section 3) and $\text{Ru}(\text{dmpe})_2(\text{CO})$ (1844 cm^{-1}).^{5a} Photolysis of $\text{Ru}(\text{dfepe})_2\text{H}_2$ in a 5% CO/Ar matrix ($\lambda = 234\text{--}376$ nm, 35 min) did not result in the formation of any new carbonyl bands. The same five-band UV-visible spectrum observed in argon and methane was found, implying that no reaction takes place at all with CO under these conditions. No changes were observed on annealing the matrix to 30 K.

2. Laser Flash Photolysis in Solution at Room Temperature. a. In the Presence of Hydrogen.

Laser flash photolysis experiments with $\text{Ru}(\text{dmpe})_2\text{H}_2$ demonstrated that $\text{Ru}(\text{dmpe})_2$ reacts with hydrogen with a second-order rate constant of $6.8 \times 10^9\text{ dm}^3\text{ mol}^{-1}\text{ s}^{-1}$ at ambient temperature.^{5a}

Laser flash photolysis ($\lambda_{\text{exc}} = 308$ nm, pulse width ca. 30 ns, pulse energy ca. 30 mJ) of $\text{Ru}(\text{depe})_2\text{H}_2$ in heptane (ca. $1.5 \times 10^{-3}\text{ mol dm}^{-3}$) at 295 K under 79 Torr of hydrogen (made up to a total pressure of 750 Torr with argon) resulted in the rapid formation (<100 ns) of a transient species at 470 nm. The transient decayed with pseudo-first-order kinetics (Figure 2a) on a microsecond time scale ($k_{\text{obs}} = 1.71 \times 10^5\text{ s}^{-1}$) restoring the original absorbance. Additional heptane solutions of the complex were made up under partial pressures of hydrogen ranging from 14 to 270 Torr with the total pressure made up to 750 Torr with argon. In all cases, the decay of the transient followed pseudo-first-order behavior and the absorbance returned to the baseline. A plot of k_{obs} versus $[\text{H}_2]$ ¹⁰ was linear (Figure 3a) and gave a second order rate constant for the reaction of $(4.0 \pm 0.4) \times 10^8\text{ dm}^3\text{ mol}^{-1}\text{ s}^{-1}$ (Table 2).

A similar series of experiments was carried out on benzene solutions of $\text{cis-Ru}(\text{dppe})_2\text{H}_2$ (ca. $6 \times 10^{-4}\text{ mol dm}^{-3}$) in the presence of hydrogen, for which a transient was observed at 460 nm. The transient decayed back to the baseline with

(9) IR bands for $\text{Ru}(\text{dfepe})_2\text{H}_2$ in an argon matrix at 12 K (ν , cm^{-1}): 1980 w, 1423 w, 1317 w, 1299 m, 1235 s, 1219 m, 1211 m, 1201 m, 1160 w, 1120 w, 1103 w, 983 w, 975 vw, 965 w, 883 vw, 823 vw.

(10) Wilhelm, E.; Battino, R. *Chem. Rev.* **1973**, *73*, 1. Gas solubilities were taken as follows: H_2 (heptane, $4.7 \times 10^{-3}\text{ mol dm}^{-3}\text{ atm}^{-1}$; benzene, $2.9 \times 10^{-3}\text{ mol dm}^{-3}\text{ atm}^{-1}$); CO (heptane, $1.2 \times 10^{-2}\text{ mol dm}^{-3}\text{ atm}^{-1}$; benzene, $7.5 \times 10^{-3}\text{ mol dm}^{-3}\text{ atm}^{-1}$); ethene (heptane, $1.2 \times 10^{-1}\text{ mol dm}^{-3}\text{ atm}^{-1}$; benzene, $1.4 \times 10^{-1}\text{ mol dm}^{-3}\text{ atm}^{-1}$).

Table 1. UV-Visible Band Maxima for Transient Species in Matrices and in Solution [λ , nm (ϵ , dm³ mol⁻¹ cm⁻¹)]^a

transient	argon matrix	methane matrix	solution
Ru(dmpe) ₂ ^b	-, 287, 463, 559, 747	-, -, 451, 543, 734	467 (2400), 555 (1700), 745 ^c (1900)
Ru(depe) ₂ ^d	-, 286, 476, 573, 757	246, 286, 476, 571, 756	475 (2500), 580 (1200), 735 ^e (630)
Ru(dppe) ₂			465, 550, 760 ^c
Ru(dfpe) ₂	251, 297, 375, 461, 611	251, 297, 375, 462, 616	380, 450, 620 ^e

^a Estimated from the kinetics in the absence of added H₂ and from the relative intensities of the bands. ^b Matrix values for Ru(dmpe)₂ for the "reversible species" taken from ref 5a. The matrix spectra also show shoulders at 365, 666 nm (Ar) and 365, 610 nm (methane). ^c Transient spectrum obtained in cyclohexane. ^d The matrix spectra show shoulders at 316, 354, 375, 665 (Ar), and 371, 665 nm (methane). ^e Transient spectrum obtained in heptane.

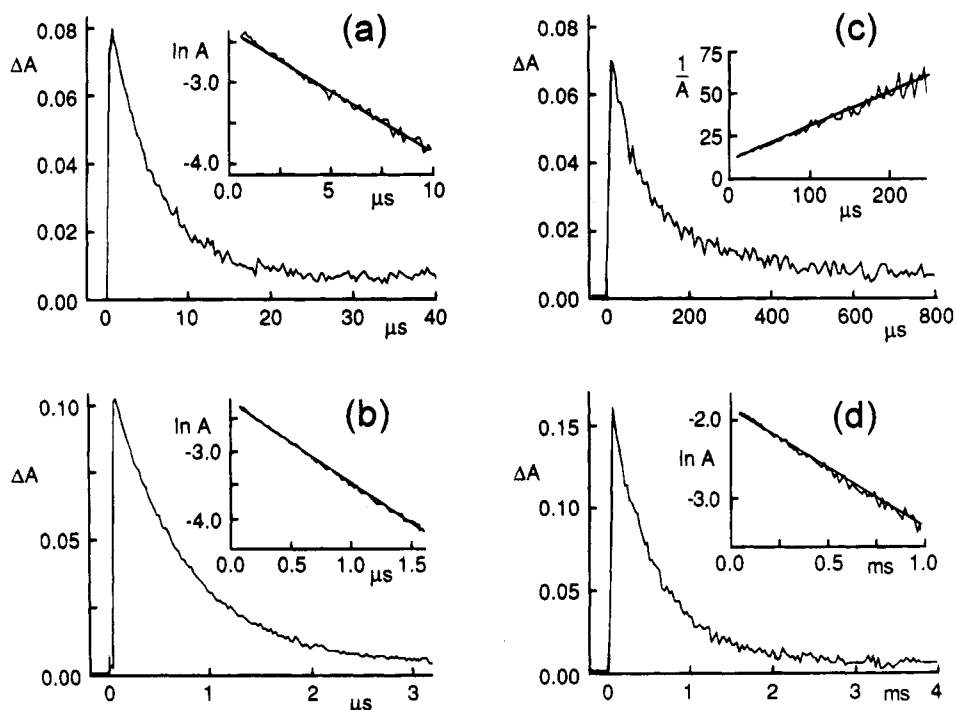


Figure 2. (a) Transient decay following laser flash photolysis (308 nm) of Ru(depe)₂H₂ in heptane solution under 79 Torr of hydrogen made up to 750 Torr with argon (the inset shows the corresponding first-order plot); (b) Transient decay and first-order plot from a similar experiment with Ru(dppe)₂H₂ in benzene solution under 760 Torr of hydrogen; (c) transient decay and second-order plot from Ru(depe)₂H₂ in heptane solution under 760 Torr of argon; (d) transient decay and first-order plot from a similar experiment with Ru(dppe)₂H₂ in benzene solution under 760 Torr of argon.

pseudo-first-order kinetics (Figure 2b) over a hydrogen partial pressure range from 80 to 760 Torr. A plot of k_{obs} versus $[\text{H}_2]$ ¹⁰ (Figure 3a) gave a second-order rate constant of $(2.4 \pm 0.2) \times 10^7 \text{ dm}^3 \text{ mol}^{-1} \text{ s}^{-1}$ (Table 2).

In the case of Ru(dfpe)₂H₂, flash photolysis of a benzene solution (ca. $8 \times 10^{-4} \text{ mol dm}^{-3}$) under 760 Torr of hydrogen resulted in the decay of a transient at 460 nm back to the baseline with pseudo-first-order kinetics over hundreds of microseconds ($k_{\text{obs}} = 5.9 \times 10^2 \text{ s}^{-1}$).

b. Transient Spectra. The spectra of the transient species formed from all three ruthenium hydride complexes were recorded under a partial pressure of hydrogen (for depe, under 11 Torr of H₂, and for dppe and dfpe, under 760 Torr of H₂) to ensure complete reversibility and prevent the build up of any stable photoproducts. For all three complexes, the transient spectra exhibited three absorption maxima between 350 and 800 nm (Figure 4, Table 1), although the central band for dppe overlapped to some extent with the highest energy band. Figure 4a shows the spectrum of Ru(dmpe)₂ for comparison. The decay kinetics of the transients were measured at each of the maxima with the same result showing that only a single intermediate was produced from each precursor. No effect of solvent (heptane, cyclohexane or benzene) was found for the transients derived from depe or dppe. Similarly the spectrum produced from Ru(dfpe)₂H₂ was the same in heptane, benzene, and perfluorohexane.

c. Flash Photolysis under Argon. Laser flash photolysis of Ru(depe)₂H₂ in heptane under argon resulted in the formation of the transient species at 470 nm, which decayed with second-order kinetics returning back to the baseline over hundreds of microseconds (slope = $k_2/\epsilon l = 2.0 \times 10^5 \text{ s}^{-1}$) (Figure 2c). The same second-order decay was observed upon changing the solvent to either cyclohexane or benzene. An increase in the concentration of precursor by a factor of 2 or 5 (achieved with different path length cuvettes but constant precursor absorbance) resulted in a more rapid decay of the transient that could not be fitted to either second-order or first-order kinetics and which no longer returned to the baseline.

Flash photolysis of a benzene solution of Ru(dfpe)₂H₂ under argon yielded a transient (at 460 nm) which also decayed with second order kinetics back to the baseline, but over a period of seconds ($k_2/\epsilon l = 1.0 \times 10^2 \text{ s}^{-1}$).

In the case of Ru(dppe)₂H₂, flash photolysis of a benzene solution under argon produced a transient species at 470 nm which decayed with pseudo-first-order kinetics over a millisecond time scale ($k_{\text{obs}} = 1.5 \times 10^3 \text{ s}^{-1}$, Figure 2d). The same observed rate constant, k_{obs} , was found upon changing the solvent to either THF or cyclohexane. The ground-state UV-visible spectrum of the solution in all solvents was changed after 200 laser shots with a new absorption band present at 375 nm. When different path length cuvettes were used in order to

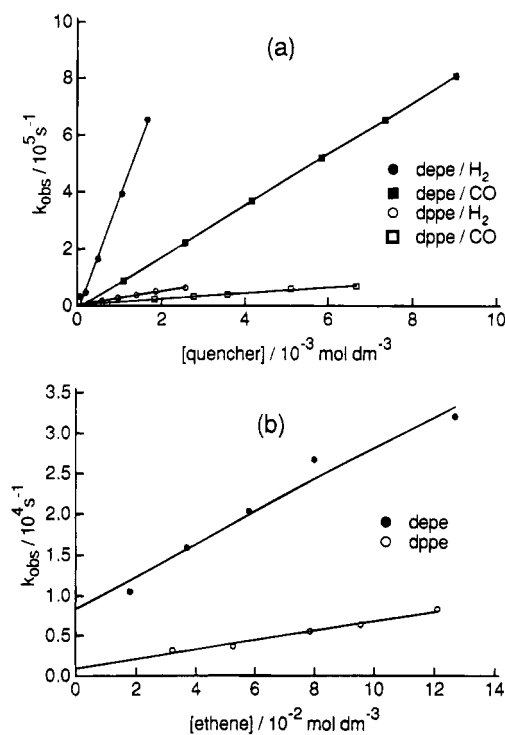


Figure 3. Plots of pseudo-first-order rate constants for the decays of the transients obtained upon laser flash photolysis of $\text{Ru}(\text{depe})_2\text{H}_2$ and $\text{Ru}(\text{dppe})_2\text{H}_2$ vs the concentration of added quenching gas for (a) H_2 and CO and (b) C_2H_4 . The best straight lines are shown as full lines through the experimental points.

Table 2. Second-Order Rate Constants^a for Reactions of Transient Species at 295 K

quencher	$k_2, \text{dm}^3 \text{mol}^{-1} \text{s}^{-1}$		
	$\text{Ru}(\text{depe})_2^b$	$\text{Ru}(\text{dppe})_2^c$	$\text{Ru}(\text{dfpe})_2^d$
H_2	$(4.0 \pm 0.4) \times 10^8$	$(2.4 \pm 0.2) \times 10^7$	2.0×10^5
CO	$(9.1 \pm 0.7) \times 10^7$	$(1.0 \pm 0.2) \times 10^7$	1.1×10^4
C_2H_4	$(2.0 \pm 0.7) \times 10^5$	$(5.9 \pm 1.9) \times 10^4$	
Et_3SiH	$(1.1 \pm 0.2) \times 10^5$		

^a Errors are shown as 95% confidence limits. ^b Data recorded in heptane. ^c Data recorded in benzene. ^d Measurement at only one gas pressure in benzene.

increase the concentration of $\text{Ru}(\text{dppe})_2\text{H}_2$ by a factor of 10, an increase in k_{obs} resulted.

d. Addition of Quenching Ligands. i. Carbon Monoxide.

Flash photolysis in the presence of CO resulted in rapid quenching of the transients from both depe (in heptane) and dppe (in benzene) and traces which no longer returned back to the baseline. Plots of k_{obs} against $[\text{CO}]$ were linear¹⁰ (Figure 3a) and gave second-order rate constants for $\text{Ru}(\text{depe})_2\text{H}_2$ of $(9.1 \pm 0.7) \times 10^7 \text{ dm}^3 \text{mol}^{-1} \text{s}^{-1}$ and $(1.0 \pm 0.2) \times 10^7 \text{ dm}^3 \text{mol}^{-1} \text{s}^{-1}$ for $\text{Ru}(\text{dppe})_2\text{H}_2$ (Table 2). For dfpe, the decay of the transient in benzene solution at 460 nm under 760 Torr of CO followed pseudo-first-order kinetics though still over hundreds of microseconds ($k_{\text{obs}} = 8.0 \times 10^1 \text{ s}^{-1}$). From this measurement at a single CO pressure, the estimated second-order rate constant was $1.1 \times 10^4 \text{ dm}^3 \text{mol}^{-1} \text{s}^{-1}$. Exposure of the sample to 100 laser shots resulted in a significant change in the ground-state UV-visible spectrum of the sample. The benzene was removed and the residue was redissolved in heptane. An IR spectrum of this sample showed bands at 1999, 2019, and 2068 cm^{-1} , which can be assigned to $\text{Ru}(\text{dfpe})_2(\text{CO})_3$.^{6g}

ii. Other Quenching Ligands. The effect of ethene on the transient kinetics was investigated for the depe and dppe

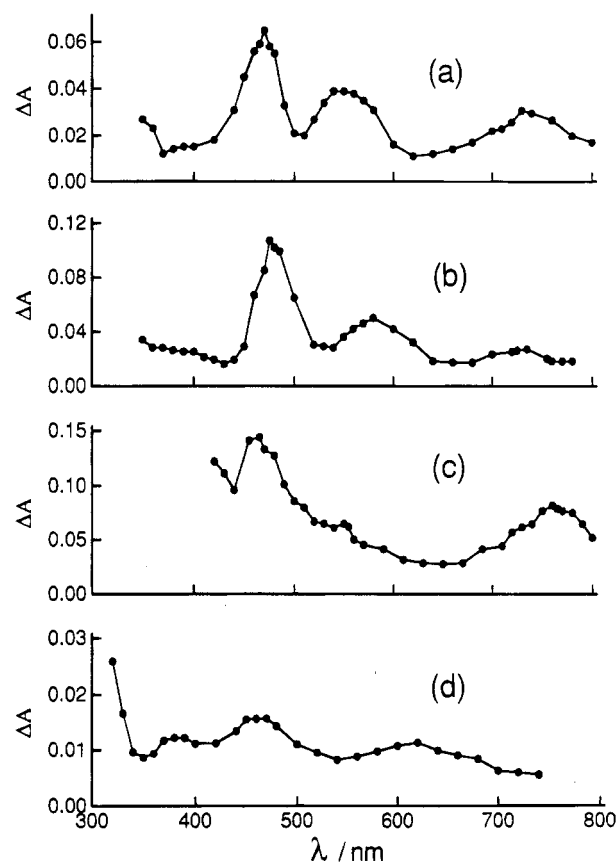


Figure 4. Transient UV-visible spectra measured at 295 K obtained 400 ns after laser flash photolysis: (a) spectrum of $\text{Ru}(\text{dmpe})_2$ in cyclohexane from ref 19b; (b) spectrum after photolysis of $\text{Ru}(\text{depe})_2\text{H}_2$ in heptane under 11 Torr of hydrogen (made up to 750 Torr with argon); (c) spectrum after photolysis $\text{Ru}(\text{dppe})_2\text{H}_2$ in cyclohexane under 760 Torr of hydrogen; (d) spectrum after photolysis of $\text{Ru}(\text{dfpe})_2\text{H}_2$ in heptane under 760 Torr of hydrogen.

complexes. Similar results were obtained to both the H_2 and CO quenching data with values of second-order rate constants for depe and dppe with ethene¹⁰ of $(2.0 \pm 0.7) \times 10^5 \text{ dm}^3 \text{mol}^{-1} \text{s}^{-1}$ and $(5.9 \pm 1.9) \times 10^4 \text{ dm}^3 \text{mol}^{-1} \text{s}^{-1}$, respectively (Figure 3b, Table 2). Addition of Et_3SiH ($2.4 \times 10^{-2} - 2.4 \text{ mol dm}^{-3}$) to heptane solutions of $\text{Ru}(\text{depe})_2\text{H}_2$ resulted in quenching of the transient as monitored at 470 nm. A plot of k_{obs} versus $[\text{Et}_3\text{SiH}]$ showed a linear dependence (Figure 5a) with a value for the second-order rate constant of $(1.1 \pm 0.2) \times 10^5 \text{ dm}^3 \text{mol}^{-1} \text{s}^{-1}$ (Table 2). The temperature dependence for the pseudo-first-order rate constant was measured over the range 303–338 K with a concentration of Et_3SiH of 0.41 mol dm^{-3} (Table 3). The activation parameters obtained were as follows: $E_a = 13.3 \pm 1.2 \text{ kJ mol}^{-1}$, $\Delta H^\ddagger = 10.6 \pm 1.3 \text{ kJ mol}^{-1}$, and $\Delta S^\ddagger = -112 \pm 4 \text{ J mol}^{-1} \text{K}^{-1}$ (Figure 5b).

Addition of Et_3SiH (up to 1.41 mol dm^{-3}) to benzene solutions of $\text{Ru}(\text{dppe})_2\text{H}_2$ did not result in any increase in the rate of decay of the transient. $\text{Ru}(\text{dfpe})_2\text{H}_2$ showed a remarkable lack of reactivity toward any added ligands. High concentrations of Et_3SiH (3.8 mol dm^{-3}) or cyclopentene (3 mol dm^{-3}) had no effect. Flash photolysis of a benzene solution of dfpe under 760 Torr of N_2 showed no evidence for reaction with nitrogen.

3. Solution Photochemistry of $\text{Ru}(\text{depe})_2\text{H}_2$, $\text{Ru}(\text{dppe})_2\text{H}_2$, and $\text{Ru}(\text{dfpe})_2\text{H}_2$. In order to interpret the results of the laser flash photolysis experiments, the photochemistry of the three complexes was probed in solution using NMR and IR studies.

Steady-state photolysis of $\text{Ru}(\text{depe})_2\text{H}_2$ in benzene- d_6 in an ampule ($\lambda > 285 \text{ nm}$, 14 h) at room temperature yielded no

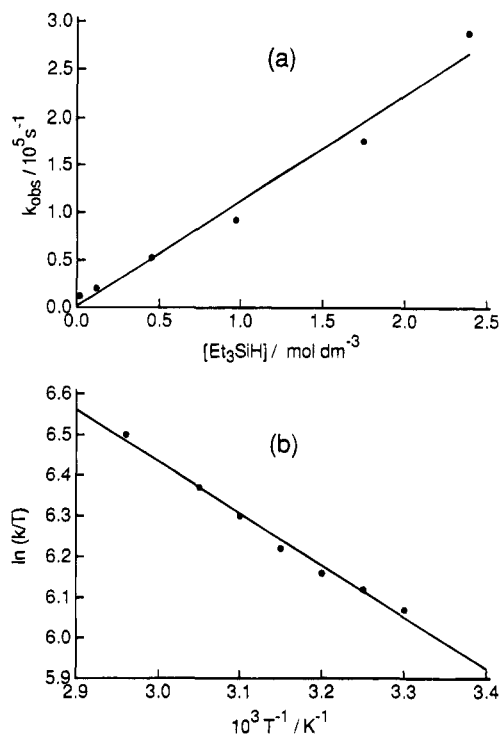
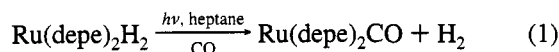


Figure 5. (a) Plot of the pseudo-first-order rate constants for the decay of the transient obtained upon laser flash photolysis of $\text{Ru}(\text{depe})_2\text{H}_2$ in heptane solution vs concentration of added triethylsilane and (b) Eyring plot of the pseudo-first-order rate constants for the same reaction in the presence of 0.41 mol dm^{-3} Et_3SiH ; $\Delta H^\ddagger = 10.6 \pm 1.3 \text{ kJ mol}^{-1}$, $\Delta S^\ddagger = -112 \pm 4 \text{ J mol}^{-1} \text{ K}^{-1}$.

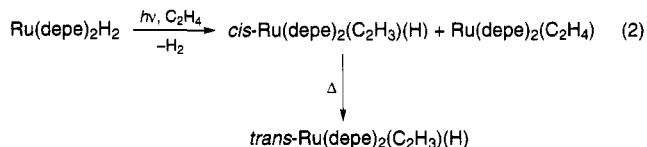
Table 3. Temperature Dependence of the Rate Constants for the Reaction of $\text{Ru}(\text{depe})_2$ with Et_3SiH (0.41 mol dm^{-3}) in heptane

Temp, K	$k_2, \text{dm}^3 \text{mol}^{-1} \text{s}^{-1}$
338	2.24×10^5
328	1.92×10^5
323	1.76×10^5
318	1.60×10^5
313	1.48×10^5
308	1.40×10^5
303	1.31×10^5

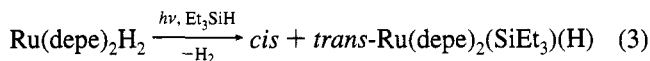
new peaks in the ^1H or $^{31}\text{P}\{^1\text{H}\}$ NMR spectra, suggesting neither activation of the solvent nor cyclometalation.¹¹ Extended photolysis in C_6H_6 or heptane was equally unproductive. Photolysis of a CO-saturated heptane solution of the dihydride in an infrared cell for 2 min resulted in the appearance of a new band at 1835 cm^{-1} in the IR spectrum, which is assigned to $\nu(\text{CO})$ of $\text{Ru}(\text{depe})_2\text{CO}$ (eq 1).



The ^1H NMR spectrum of a sample of $\text{Ru}(\text{depe})_2\text{H}_2$ in benzene- d_6 after photolysis under 760 Torr of ethene ($\lambda > 285 \text{ nm}$, 12 h) showed a new hydride resonance at $\delta -10.4$ (dq, $J_{\text{PH}} = 72.1$ and 24.1 Hz) together with new multiplets at $\delta 5.95$, 6.79 , and 7.82 , consistent with the presence of a vinyl group. The resonance at lowest field showed a characteristic $J_{\text{H-H}}$ coupling of 18.7 Hz and additional couplings to phosphorus suggesting assignment to the α -vinyl proton. The $^{31}\text{P}\{^1\text{H}\}$ NMR spectrum displayed four resonances in an ABMQ pattern. The proton spectrum is close to that previously reported for *cis*- $\text{Ru}(\text{depe})_2(\text{C}_2\text{H}_3)\text{H}$,^{5a} and suggests formation of the corresponding *cis*- $\text{Ru}(\text{depe})_2(\text{C}_2\text{H}_3)\text{H}$.¹² A small amount of the ruthenium (0) complex, $\text{Ru}(\text{depe})_2(\text{C}_2\text{H}_4)$, was also formed. After 2 days at 5°C , the *cis* species had been depleted and a new hydride resonance had appeared at $\delta -20.68$ (q, $J_{\text{PH}} = 20.0 \text{ Hz}$). New broad vinyl resonances were also observed at $\delta 5.83$, 6.67 , and 7.69 . The $^{31}\text{P}\{^1\text{H}\}$ NMR spectrum showed a new singlet at $\delta 84.4$. The data are consistent with isomerization to the *trans*-vinyl hydride complex (eq 2).¹²



The ^1H NMR spectrum recorded following photolysis of $\text{Ru}(\text{depe})_2\text{H}_2$ in neat Et_3SiH for 14 h showed resonances for starting material along with two new ruthenium hydride resonances at $\delta -12.2$ (dq, distorted) and -22.4 (q, $J_{\text{PH}} = 19.8 \text{ Hz}$). The region associated with the Et_3Si groups was complicated by overlapping resonances. The $^{31}\text{P}\{^1\text{H}\}$ NMR spectrum contained a singlet at $\delta 64.5$ and a series of resonances showing severe second-order effects. The NMR data are consistent with the formation of both *cis*- and *trans*-silyl hydride species. Photolysis for 2 h resulted in very low conversion of starting material but resonances for both the *cis*- and *trans*-silyl hydride complexes were already present indicating that the *cis*-isomer isomerises to the *trans*-isomer within a few hours (eq 3).



Extended photolysis of $\text{Ru}(\text{dppe})_2\text{H}_2$ in benzene- d_6 ($\lambda > 285 \text{ nm}$, 5 days) resulted in the appearance of only minor new peaks in the ^1H and $^{31}\text{P}\{^1\text{H}\}$ NMR spectra. Both Traverso and co-workers¹³ and Azizian and Morris¹⁴ have reported that irradiation of $\text{Fe}(\text{dppe})_2\text{H}_2$ in toluene solution for 3 h resulted in formation of the previously characterized cyclometalated complex, $\text{Fe}(\text{dppe})(\text{C}_6\text{H}_4\text{P}(\text{Ph})\text{C}_2\text{H}_4\text{PPh}_2)\text{H}$.¹⁵ In order to confirm the photochemical loss of hydrogen from $\text{Ru}(\text{dppe})_2\text{H}_2$, a CO-saturated toluene solution was photolyzed in an IR cell for 2 min. The IR spectrum showed depletion of the metal-hydride stretch at 1880 cm^{-1} and formation of a new, more intense band at 1847 cm^{-1} resulting from $\text{Ru}(\text{dppe})_2\text{CO}$.

Photolysis of $\text{Ru}(\text{dfpe})_2\text{H}_2$ in THF- d_8 ($\lambda > 285 \text{ nm}$, 4 h, -78°C) yielded no new peaks in the ^1H or $^{31}\text{P}\{^1\text{H}\}$ NMR spectra.

Discussion

The photochemistry of $\text{Ru}(\text{depe})_2\text{H}_2$, $\text{Ru}(\text{dppe})_2\text{H}_2$ and $\text{Ru}(\text{dfpe})_2\text{H}_2$, has been studied in solution at room temperature

(12) (a) *cis*- $\text{Ru}(\text{depe})_2(\text{C}_2\text{H}_3)\text{H}$: ^1H NMR (benzene- d_6 , 500 MHz) $\delta -10.41$ dq ($J_{\text{PHtrans}} = 72.1$, $J_{\text{PHcis}} = 24.1$), 5.95 m ($\text{RuCH}_a\text{CH}_b\text{H}_c$, $J_{\text{HaHc}} = 18.7$, $J_{\text{HbHc}} = 6.1$), 6.79 m ($\text{RuCH}_a\text{CH}_b\text{H}_c$, $J_{\text{HaHb}} = 12.0$, $J_{\text{HbHc}} = 6.1$), 7.82 m ($\text{RuCH}_a\text{CH}_b\text{H}_c$, $J_{\text{HaHc}} = 18.7$, $J_{\text{HaHb}} = 12.0$). $^{31}\text{P}\{^1\text{H}\}$ NMR (benzene- d_6 , 202 MHz) $\delta 44.0$ (P_Q), 58.0 (P_M), 65.2 (P_A), 63.8 (P_B) ($J_{\text{AB}} = 264.2$, $J_{\text{AQ}} = 19.1$, $J_{\text{AM}} = 16.2$, $J_{\text{BM}} = 20.6$, $J_{\text{BQ}} = 15.4$, $J_{\text{QM}} = 12.1$). *trans*- $\text{Ru}(\text{depe})_2(\text{C}_2\text{H}_3)\text{H}$: ^1H NMR (benzene- d_6 , 500 MHz) $\delta -20.68$ q ($J_{\text{PH}} = 20.0$), 5.83 br m, 6.67 br m, 7.69 br m. $^{31}\text{P}\{^1\text{H}\}$ NMR (benzene- d_6 , 202 MHz) $\delta 84.4$ s. (b) Isomerization of *cis*- $\text{Fe}(\text{dmpe})_2(\text{C}_2\text{H}_3)\text{H}$ to the corresponding *trans* isomer has been observed. Baker, M. V.; Field, L. D. *J. Am. Chem. Soc.* **1986**, *108*, 7436.

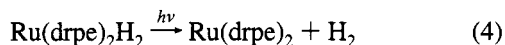
(13) Maldotti, A.; Sostero, S.; Traverso, O.; Sima, J. *Inorg. Chim. Acta* **1981**, *54*, L271.

(14) Azizian, H.; Morris, R. H. *Inorg. Chem.* **1983**, *22*, 6.

(15) Ittel, S. D.; Tolman, C. A.; Krusic, P. J.; English, A. D.; Jesson, J. P. *Inorg. Chem.* **1978**, *17*, 3432.

(11) This result contrasts with those of Baker and Field on *cis*- $\text{Fe}(\text{depe})_2(\text{CH}_3)\text{H}$, which reductively eliminates methane above 240 K to give $\text{Fe}(\text{depe})_2$. This species readily cyclometalates. Baker, M. V.; Field, L. D. *Organometallics* **1986**, *5*, 821.

by laser flash photolysis and in low temperature matrices. The results parallel those obtained earlier on Ru(dmpe)₂H₂, and are fully consistent with the formation of the 4-coordinate Ru(drpe)₂ (drpe = depe, dppe, dfep) species in the primary photochemical step (eq 4).



The reductive elimination of H₂ is complete well within the instrumental risetime (<100 ns). In the presence of added H₂, the Ru(drpe)₂ species react readily to reform the precursor. Alternatively the 16-electron intermediate may be trapped with other reagents. There are two very striking deductions from these results. Firstly, the multiband UV–visible spectrum is characteristic of all four 16-electron complexes, indicating a common molecular and electronic structure. Since detailed evidence of the crystal structure and electronic spectra are available for the isoelectronic rhodium cations, we can make very firm deductions about Ru(drpe)₂. Secondly, comparisons of rate constants for the four complexes show that rates of oxidative addition and ligand coordination are highly sensitive to substituent.

Spectra and Structure. All four Ru(drpe)₂ species show multiband UV–visible spectra. For Ru(dmpe)₂ and Ru(depe)₂, there are three prominent bands between 400 and 800 nm. In Ru(dppe)₂, the central band lies close to the high energy band and is not well resolved. The spectrum of Ru(dfep)₂ is conspicuously blue-shifted compared to all the others, so the three bands lie in the region 350–700 nm. Comparisons of the solution spectra show that the long wavelength band follows the trend in λ_{max} : Ph > Me > Et > C₂F₅ with small shifts between the first three complexes and 2500 cm⁻¹ between Ru(depe)₂ and Ru(dfep)₂. The short-wavelength band and the central band follow the trend in λ_{max} : Et > Me > Ph > C₂F₅.

We have shown previously^{5a} that there are two forms of Ru(dmpe)₂ present in an argon matrix with slightly different visible spectra, a “reversible” form in which expelled H₂ is held close by in the matrix cage, and an “irreversible” form in which the hydrogen molecule has diffused out of the cage. In the case of Ru(depe)₂, we only observed a reversible form whereas Ru(dfep)₂ failed to recombine with H₂ altogether.

We postulated previously that the multiband spectrum of Ru(dmpe)₂ is characteristic of a square-planar geometry and that the lowest energy band should be assigned to a metal-centered d_{z²}-p_z transition. We were hampered in comparisons with the literature because there are few spectra of square-planar complexes with σ -bonding ligands only, and those did not show a comparable pattern of bands. The present results demonstrate that Ru(depe)₂ and, most importantly, Ru(dppe)₂, must have the same electronic and molecular structure as Ru(dmpe)₂. The isoelectronic ion, [Rh(dppe)₂]⁺, has been shown crystallographically to adopt a structure close to square planar.¹⁶ Geoffroy et al.¹⁷ carried out a thorough investigation of the UV–visible and MCD spectra of salts of [M(dppe)₂]⁺ (M = Rh, Ir) and found three bands for each salt with extinction coefficients above 4000 dm³ mol⁻¹ cm⁻¹ between 22 000 and 32 000 cm⁻¹ (the central rhodium band required MCD in order to pick it out from the high energy band). The longest wavelength band was assigned to a ¹A_{2u} excited state on the basis of the sign of the dichroism. In the Rh complex, complications from spin-orbit coupling are

not very important. The ¹A_{2u} excited state must arise from an a_{1g}(d_{z²}) to a_{2u} transition (assuming approximate D_{4h} symmetry). Geoffroy et al.¹⁷ visualized the a_{2u} orbital as a mixture of M(p_z), ligand P(3d) and ligand π^* . In examining our own results, we see a very close analogy with the spectra of [Rh(dppe)₂]⁺. The same three band pattern is observed for Ru(dppe)₂, but the bands are shifted 11000–12000 cm⁻¹ to lower energy compared to the rhodium cation. Since we observed the same pattern for the dmpe and depe compounds, we can be certain that ligand π^* orbitals do not play an essential role in generating this type of spectrum. According to current understanding, the role of P(3d) orbitals is also likely to be minor. We thus assign the lowest energy transition as predominantly M(d_{z²}) to M(p_z). The higher energy bands probably involve the remaining occupied d orbitals. In D_{4h} symmetry, only one additional transition is allowed, viz. from e_g (d_{xz,yz}) to a_{2u}(p_z). However, on reducing the symmetry to D_{2h}, allowed transitions are predicted from each of the occupied d orbitals to the p_z orbital which now has b_{1u} symmetry. Since the degeneracy of d_{xz} and d_{yz} is lifted, there are a total of four allowed transitions.

There are several related observations which support the structural and spectroscopic arguments. Firstly, Ru(CO)₂(PMe₃)₂ and RuP(CH₂CH₂PPh₂)₃ do not exhibit the three-band UV–visible spectrum,^{18,19a} but each shows a single band in the region 380–430 nm. Since neither complex is square planar, we see that the multiband spectrum is lost on changing the geometry. Secondly, density functional calculations on Ru(PH₃)₄ and [Rh(PH₃)₄]⁺ predict structures with D_{2d} symmetry which are close to square planar (PMP angles of 165° and 170° for Ru and Rh⁺, respectively).²⁰ By analogy with experimental structures^{21,22} of [Rh(PMe₃)₄]⁺ and [Rh(dmpe)₂]⁺, chelation forces the RhP₄ skeleton to be planar. The calculations predict a d_{z²}-p_z excitation energy of 14 900 cm⁻¹ for Ru(PH₃)₄ rising to 22 800 cm⁻¹ for [Rh(PH₃)₄]⁺, in excellent agreement with experiment.²⁰

The spectra of Ru(dmpe)₂, Ru(depe)₂, and Ru(dppe)₂ are extremely similar to one another in keeping with transitions which are predominantly metal centered. Thus there is no evidence for agostic interactions between a phenyl group and the metal. The bands of Ru(dfep)₂ are all significantly blue-shifted relative to the other RuP₄ complexes. The high energy shifts could arise from a slight distortion away from square-planar geometry,²⁰ or from coordination of fluorine to the metal via one of the C₂F₅ groups (see below). However, either of these effects would have to be slight, otherwise the three band pattern would be destroyed as in Ru(CO)₂(PMe₃)₂. It is noticeable that Ru(dfep)₂ is closer in geometry to Ru(dmpe)₂ than to Ru(CO)₂(PMe₃)₂ or Ru(CO)₄ (predicted to adopt a C_{2v} structure).²³ The electronic characteristics of dfep should mimic those of CO,²⁴ although a recent ligand effect study places

(18) Mawby, R. J.; Perutz, R. N.; Whittlesey, M. K. *Organometallics* **1995**, *14*, 3268.

(19) (a) Osman, R. D.Phil. Thesis, University of York, 1993. (b) The spectrum of Ru(dmpe)₂ was obtained after flash photolysis of Ru(dmpe)₂(C₂H₄). The band positions are identical to those obtained from photolysis of Ru(dmpe)₂H₂.

(20) Macgregor, S. A.; Eisenstein, O.; Whittlesey, M. K.; Perutz, R. N. Manuscript in preparation. The calculations showed that the d_{z²}-p_z transition of Ru(PH₃)₄ lies at 14 900 cm⁻¹ in the equilibrium geometry with PRuP angles of 165°, but at 14 100 cm⁻¹ in a square-planar geometry.

(21) Jones, R. A.; Real, F. M.; Wilkinson, G.; Galas, A. M. R.; Hursthouse, M. B. *J. Chem. Soc., Dalton Trans.* **1980**, 511.

(22) Marder, T. B.; Williams, I. D. *J. Chem. Soc., Chem Commun.* **1987**, 1478.

(23) (a) Ziegler, T.; Tshinke, V.; Fan, L.; Becke, A. D. *J. Am. Chem. Soc.* **1989**, *111*, 9177. (b) Li, J.; Schreckenbach, G.; Ziegler, T. *J. Am. Chem. Soc.* **1995**, *117*, 486.

(24) (a) Ernst, M. F.; Roddick, D. M. *Inorg. Chem.* **1989**, *28*, 1624. (b) Roddick, D. M.; Schnabel, R. C. *ACS Symp. Ser.* **1994**, *555*, 421.

(16) Hall, M. C.; Kilbourn, B. T.; Taylor, K. A. *J. Chem. Soc. (A)* **1970**, 2539. The deviations of the RhP₄ atoms from the mean plane are ca. 0.04 Å. The mean intraligand PRhP angles are 82.7°. The mean PRhP (trans) angles are 176.9°.

(17) Geoffroy, G. L.; Isci, H.; Litrenti, J.; Mason, W. R. *Inorg. Chem.* **1977**, *16*, 1950.

2nd Order Rate Constants

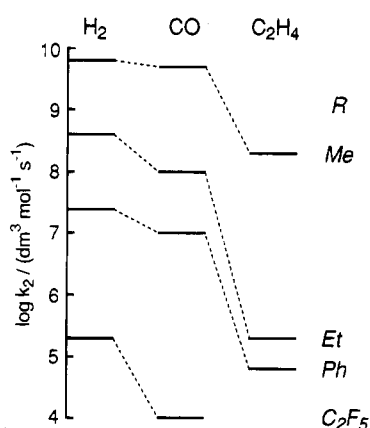


Figure 6. Schematic comparison of the reactivities of Ru(drpe)₂ (drpe = dmpe, depe, dppe, and dfepe) with hydrogen, CO, and ethene expressed as log k_2 where k_2 are the second-order rate constants.

Experimental Section

General Methods and Materials. Ruthenium trichloride, depe, and dppe were obtained from Aldrich. Compounds were synthesized and handled using standard Schlenk, high-vacuum, and glovebox techniques. Solvents for synthesis (AR Grade) were dried by refluxing over sodium/benzophenone (benzene, hexane, toluene, THF) or P₂O₅ (CH₂Cl₂) and then distilled under an argon atmosphere while those for flash photolysis (Aldrich HPLC Grade) were refluxed over calcium hydride under argon. Perfluorohexane (Aldrich, 95%) was distilled from CaH₂ under argon. Benzene-*d*₆ and THF-*d*₈ (Goss Scientific Instruments Ltd.) were dried by stirring over potassium/benzophenone and then vacuum transferred. Hydrogen used in synthesis was BOC standard grade (99.9% purity). Gases used for the matrix experiments (Ar, CH₄, CO) and for flash experiments (Ar, H₂, CO, N₂, C₂H₄) were BOC research grade (99.999% purity). Triethylsilane was stored over activated 3 Å molecular sieves.

Matrix Isolation Experiments. The matrix isolation apparatus is described in detail elsewhere.³¹ Samples for IR spectroscopy alone were deposited onto a CsI window cooled by an Air Products CS202 closed-cycle refrigerator to 12–35 K. A BaF₂ window was used for combined IR and UV–visible spectroscopy. The outer windows of the vacuum shroud were chosen to match. Ru(depe)₂H₂ and Ru(dfep)₂H₂ were sublimed from right-angled glass tubes (at 388 and 358 K, respectively) at the same time as a gas stream entered the vacuum shroud through a separate inlet. Typical deposition temperatures and rates were 20 K for Ar (2 mmol h⁻¹) and 25 K for CH₄ (2 mmol h⁻¹). The samples were then cooled to 12 K before recording IR spectra on a Mattson Research Series FTIR spectrophotometer fitted with a TGS detector and KBr beam splitter, which was continuously purged with dry CO₂-free air. Spectra were recorded at 1 cm⁻¹ resolution with 128 scans coaveraged (25K data points with two-times zero filling). UV–visible spectra were recorded on the same sample at the same temperature on a Perkin-Elmer Lambda 7G spectrophotometer. Matrices were photolyzed through a quartz window with a

Philips HPK 125-W medium-pressure mercury arc, quartz focusing lens and water filter or with an ILC 302UV 300 W Xe arc equipped with either UV-reflecting (240–400 nm) or with visible-reflecting (400–800 nm) mirrors and a water filter. Photolysis wavelengths were selected with cutoff or interference filters.

Laser Flash Photolysis. The apparatus for flash photolysis experiments has been described in detail elsewhere.⁵ Briefly, a XeCl excimer laser (308 nm) is used as the excitation source and a pulsed Xe arc lamp is used as the monitoring source. The spectrometer is linked to a digital oscilloscope, and the system is controlled by a PC. Transient signals are usually collected as 12- or 16-shot averages. Some of the data for Ru(dfep)₂H₂ were collected on a similar apparatus at the University of Ottawa.

Samples of Ru(dfep)₂H₂ for flash experiments were sublimed immediately before use, and Ru(depe)₂H₂ and Ru(dppe)₂H₂ were freshly recrystallized. Samples of the depe complex were handled in the glovebox exclusively. The samples were loaded into a quartz cuvette (1-, 2-, or 10-mm pathlength) fitted with a Young's PTFE stopcock and degassing bulb. Solvent was added via a cannula under argon on a Schlenk line fitted with a diffusion pump. The sample was degassed three times by freeze–pump–thaw cycles before being back-filled to 760 Torr with the appropriate gas. Gas mixtures were made up manometrically in 1-L bulbs such that the total pressure in the cell was typically 750 Torr. Liquid quenchers were added with a microliter syringe. The absorbances of the samples were typically 0.5–1.0 at 308 nm. Variable-temperature measurements were made by replacing the standard cell holder by an insulated holder mounted on a block through which thermostated water was passed.

NMR Spectroscopy. The NMR spectra were recorded with either Bruker MSL300 or AMX500 spectrometers. The ¹H NMR chemical shifts were referenced to residual C₆D₅H at δ 7.13 ppm. The ³¹P{¹H} NMR chemical shifts were referenced externally to H₃PO₄ at δ = 0.

Synthesis. *trans*-Ru(depe)₂Cl₂,³² Ru(dppe)₂H₂,³³ and Ru(dfep)₂H₂⁶⁸ were prepared by literature methods.

***cis*-Ru(depe)₂H₂.** *trans*-Ru(depe)₂Cl₂ (300 mg, 0.51 mmol) was dissolved in 20 mL of THF. Freshly cut Na (300 mg) was added, and the mixture was stirred under 760 Torr of H₂ in an ampule for 24 h at room temperature. The solvent was then removed from the resulting gray suspension and the residue extracted exhaustively with hexane (3 × 20 mL) and filtered through Celite to yield a colorless solution. After the solution was cooled to –20 °C overnight, white crystals of Ru(depe)₂H₂ were obtained; yield 200 mg (84%). The NMR data were consistent with the literature.³³ The ³¹P{¹H} NMR spectrum showed a 3:1 ratio of *cis/trans* species.

Acknowledgment. We are extremely grateful to D. Dukic for his help in interfacing and development of the software for the flash photolysis apparatus. We are pleased to acknowledge the support of SERC, the European Commission, NATO, British Gas, Johnson Matthey, The Royal Society, and NSF.

JA951997M

(32) Chatt, J.; Hayter, R. G. *J. Chem. Soc.* **1961**, 896.

(33) Bautista, M. T.; Cappellani, E. P.; Drouin, S. D.; Morris, R. H.; Schweitzer, C. T.; Sella, A.; Zubkowski, J. *J. Am. Chem. Soc.* **1991**, *113*, 4876.

(31) Haddleton, D. M.; McCamley, A.; Perutz, R. N. *J. Am. Chem. Soc.* **1988**, *110*, 1810.